JCSE The Journal of Corrosion Science and Engineering
ISSN 1466-8858 Volume 11, Preprint 11 submitted 30 August 2008

# On the Nature of Rusts on Phosphoric Irons

Gadadhar Sahoo[a], R. Balasubramaniam[b] and A. C. Vajpei[b]
[a]R & D Centre for Iron and Steel, Steel Authority of India Limited, Ranchi 834002, India
gadadharsahoo@yahoo.com
[b]Department of Materials and Metallurgical Engineering, Indian Institute of Technology, Kanpur 208016, India, bala@iitk.ac.in

## Abstract

Rusts from three phosphorus containing irons or phosphoric irons (Fe-0.11P-0.028C, Fe-0.32P-0.026C and Fe-0.49P-0.022C, all in wt. %), after exposure to one year in the atmosphere, 15 days in continuous salt spray and 20 days in cyclic wet-dry salt spray, were analyzed using X-ray diffraction and Fourier transform infrared spectroscopy. They were found to be similar in nature to rusts on a plain carbon steel (Fe-0.148 C-0.542 Mn-0.128 Si) and a microalloyed steel (Fe-0.151C-0.088P-0.197Si-0.149Cr-0.417Cu). Polarization study of one-year atmosphere exposed samples in 3.5 % NaCl solution did not reveal beneficial effect of phosphorus in phosphoric irons. However, the improved corrosion resistance of phosphoric irons in chloride-containing environments was concluded based on electrochemical impedance studies on rusted surfaces. In case of salt spray exposed samples, the polarization resistance of phosphoric irons increased with increasing phosphorus content and was higher than that of plain carbon steel and microalloyed steel.

**Keywords**: Phosphoric irons, Rust characterization, X-ray diffraction, FTIR, EIS, Polarization.

## 1.0 Introduction

The 1600-year old Delhi Iron Pillar is well known for its remarkable corrosion resistance. This exceptional corrosion resistance arises due to the presence of relatively high phosphorus content (0.25 wt-%) in the Pillar. Phosphorus plays a major role by facilitating the formation of a protective passive film on the surface [1, 2]. Based on the example of Delhi Iron Pillar, a detailed study on the corrosion behavior of phosphoric irons (i.e. phosphorus containing irons) was undertaken [3]. The significant conclusion derived was that phosphoric irons possessed better corrosion resistance than conventional steels used in concrete environment [3]. The required strengths and ductility have been obtained in phosphoric irons by controlling chemistry and microstructure [4]. Therefore, phosphoric irons are candidate materials for concrete reinforcement application.

ISSN 1466-8858 Volume 11, Preprint 11 submitted 30 August 2008

It is important to understand the nature of rusts that form on phosphoric irons and compare them with rusts on normal steels, preferably those used in concrete reinforcement applications. The aim of the present study was first, to characterize the rusts developed on phosphoric irons and commercial concrete reinforcement steels after one year of atmospheric exposure, and short duration exposure to continuous and cyclic wet-dry salt spray conditions using spectroscopic techniques. The second aim was to estimate the corrosion resistance of rust covered surfaces using electrochemical techniques.

## 2.0 Experimental

Phosphoric irons of three different phosphorus contents, namely $P_1$, $P_2$ and $P_3$, were prepared by ingot casting route after melting in a high frequency induction-melting furnace (175 KW, 1000 Hz, Inductotherm, India Pvt. Ltd.) in air. The alloys were prepared from calculated amounts of soft iron (Fe-0.001C) and Fe-P mother alloys (Fe-22P). The carbon content was controlled to about 0.02 wt. % by addition of mild steel scraps containing 0.16 % carbon. The ingots were soaked and then forged at 1150$^0$C into round bars of 26 mm diameter. Two commercial concrete reinforcement steels named as T and C, both of 22 mm diameter, were used as reference. Sample T was a plain carbon steel while C was a microalloyed steel. The chemical compositions of $P_1$, $P_2$, $P_3$, T and C were obtained in an optical emission spectrometer (BAIRD SPECTRO VAC DV-6, USA) and are provided in Table 1. The chemical compositions of phosphorus in phosphoric irons were determined by wet chemical analysis.

Table 1: Average chemical compositions of phosphoric irons, T and C (weight %).

| Samples | C | P | Si | Mn | S | Ni | Cr | Mo | V | Cu |
|---|---|---|---|---|---|---|---|---|---|---|
| $P_1$ | 0.028 | 0.11 | 0.029 | 0.046 | 0.017 | 0.026 | 0.044 | 0.004 | 0.003 | 0.033 |
| $P_2$ | 0.026 | 0.32 | 0.026 | 0.052 | 0.018 | 0.026 | 0.045 | 0.004 | 0.004 | 0.036 |
| $P_3$ | 0.022 | 0.49 | 0.027 | 0.067 | 0.023 | 0.026 | 0.056 | 0.004 | 0.004 | 0.038 |
| T | 0.148 | 0.024 | 0.128 | 0.542 | 0.02 | <0.011 | 0.036 | 0.002 | 0.003 | 0.012 |
| C | 0.151 | 0.088 | 0.197 | 0.713 | 0.013 | <0.011 | 0.149 | 0.004 | 0.004 | 0.417 |

JCSE The Journal of Corrosion Science and Engineering
ISSN 1466-8858 Volume 11, Preprint 11 submitted 30 August 2008

## 2.1 Atmospheric Exposure Testing

Atmospheric exposure tests were performed according to ASTM G 50-76. An exposure rack of mild steel was fabricated. This was placed on the roof of Western Laboratory, IIT Kanpur, Kanpur ($80^0$ 20' E and $26^0$ 26' N), an urban industrial location in Northern India. The location was a clear, well drained area. It was ensured that shadows of trees, buildings, or structures did not fall on the specimens. The specimens were suspended at an angle of $45^0$. The suspended specimens during exposure test are shown in Figure 1 after one year of exposure to atmosphere environment.

Figure 1: Samples suspended on rack during atmosphere exposure testing.

The 22 mm diameter sample rods were machined and surface finished with 120 grit SiC abrasive paper before exposure. The samples were exposed on the 22nd of November 2004 and removed, for rust analysis and electrochemical tests, on the 30th of November 2005. The temperatures of the atmosphere of Kanpur during this period (for 1 h interval) were obtained from the Chakeri Air Force Station (Meteorological Section), Kanpur.

One set of specimens was removed from the second row for rust analysis and electrochemical tests. Other samples are still exposed for long term testing.

Rusts were collected from specimens in the second row by scraping, using a stainless steel spatula. The rusts at top and bottom of each rod were kept intact. Specimens of 5 mm

ISSN 1466-8858 Volume 11, Preprint 11 submitted 30 August 2008

length were cut from the top and bottom portions of rods by an electric abrasive cutter. These samples were used for polarization experiments in 3.5 % NaCl for evaluating the electrochemical nature of the rusted surfaces. The polarization experiments were conducted in a standard flat cell (Princeton Applied Research, Ametek, USA) in the potential range -250 mV to 250 mV versus open circuit potential of samples, using 263A potentiostat (Princeton Applied Research, Ametek, USA). A calomel electrode was used as reference electrode. The scan rate employed for the polarization studies was 0.166 $mVs^{-1}$. The linear cathodic portion of the polarization curve was extrapolated to the horizontal drawn at the zero current potential to obtain the $i_{corr}$ [5].

## 2.2 Salt Spray Testing

All samples were subjected to salt spray testing for 15 days, according to ASTM B117-03. A salt solution of 5-wt % was prepared using distilled water. The temperature of salt spray chamber was maintained at $35^0$C. The samples were prepared as thin slices of about 6 mm thickness along transverse direction of the 16 mm diameter bars. Each slice was mounted in cold setting epoxy. An insulated wire was connected to the samples before setting in epoxy to facilitate hanging of samples inside salt spray chamber. The samples were polished using 120 grit silicon carbide abrasive paper. The samples were suspended in the chamber at an angle of $30^0$ from vertical. Samples were periodically removed (1d and 15d) from the salt spray chamber for conducting electrochemical impedance test in 3.5 % NaCl using a standard flat cell (Princeton Applied Research, Ametek, USA) having 1 $cm^2$ exposed area facility for the specimen.

EIS scan was carried out by applying a sinusoidal potential perturbation of 10 mV at the open circuit potentials with frequency sweep from 100 kHz to 5 mHz using PARSTAT 2263 potentiostat and PowerSuit software (Princeton Applied Research, Ametek, USA).

Another set of samples, of 10 cm length and 10 mm diameter, were suspended for collecting rust for analysis. These samples were surface finished using 120 grit silicon carbide paper before exposure. Rusts were collected from the surface of these samples after 15 days and characterized by X-ray diffraction (XRD) using Cu target and Fourier transform infrared (FTIR) spectroscopy.

The salt spray test chamber was also used to simulate wet-dry exposure. Two sets of samples were subjected to alternate wet (at $35^0$C) and dry (at $60^0$C) conditions with a wet dry ratio of 2:6 hours for a total period of 20 days. One set of samples was connected with insulated wire and mounted in cold setting epoxy, in the way similar to that was done in the

JCSE The Journal of Corrosion Science and Engineering
ISSN 1466-8858 Volume 11, Preprint 11 submitted 30 August 2008

case of continuous salt spray exposure test. The other set of samples were rods of 10 cm length and 10 mm diameter. The samples used in this test were surface finished in a manner described earlier for continuous-exposure salt spray testing. While EIS scans were obtained in 3.5 % NaCl solution for one set of epoxy-mounted samples, rusts were collected from the other set of samples for further analysis.

## 3.0 Results and Discusion

### 3.1 Atmospheric Exposure Test

The temperature of Kanpur was averaged out for each month and the average temperature data is shown in Figure 2.

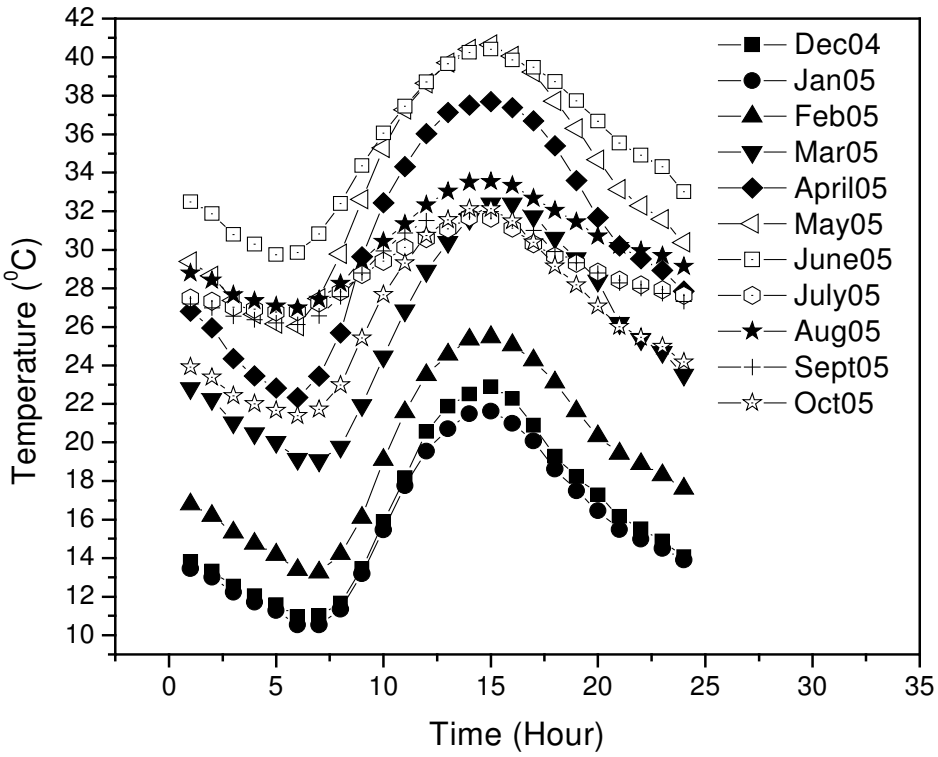


Figure 2: Variation of temperature of Kanpur for 11 month period between December 2004 and October 2005.

JCSE The Journal of Corrosion Science and Engineering
ISSN 1466-8858 Volume 11, Preprint 11 submitted 30 August 2008

The monthly average relative humidity at Kanpur during this period is shown in Figure 3.

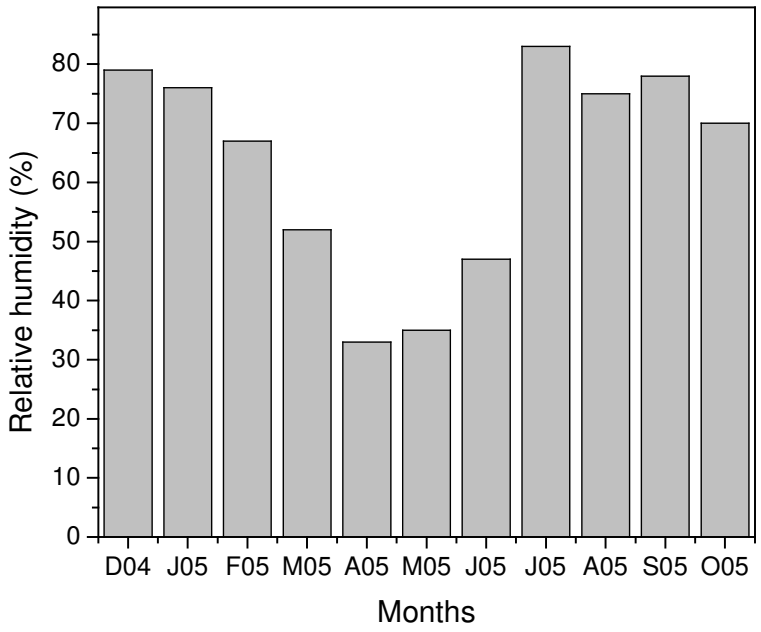


Figure 3: Variation of monthly average relative humidity at Kanpur for 11 month period between December 2004 and October 2005.

It is to be noted that the humidity level is low in the summer season in India during the months of March, April, May and June. As shown in Figure 3, these values are lower than 60 % for the above four months. The atmospheric corrosion of iron becomes significant for relative humidity beyond 60 % [6], conditions favourable for atmospheric corrosion existed at Kanpur for significant period (almost 8 months) in the year. As shown in the Figure 3, the average humidity level of above 60 % for the month of July, August and September can be attributed to the rainy season. The humidity level is also high during the winter months due to the cold weather.

The color of the rust on each specimen, after the atmospheric exposure, was different (Figure 4). The rusts appeared dark reddish brown both in T and C, while those on phosphoric irons were lighter. Among phosphoric irons, the colour of the rust in $P_3$ was more reddish than that in $P_1$ and $P_2$.

JCSE The Journal of Corrosion Science and Engineering
ISSN 1466-8858 Volume 11, Preprint 11 submitted 30 August 2008

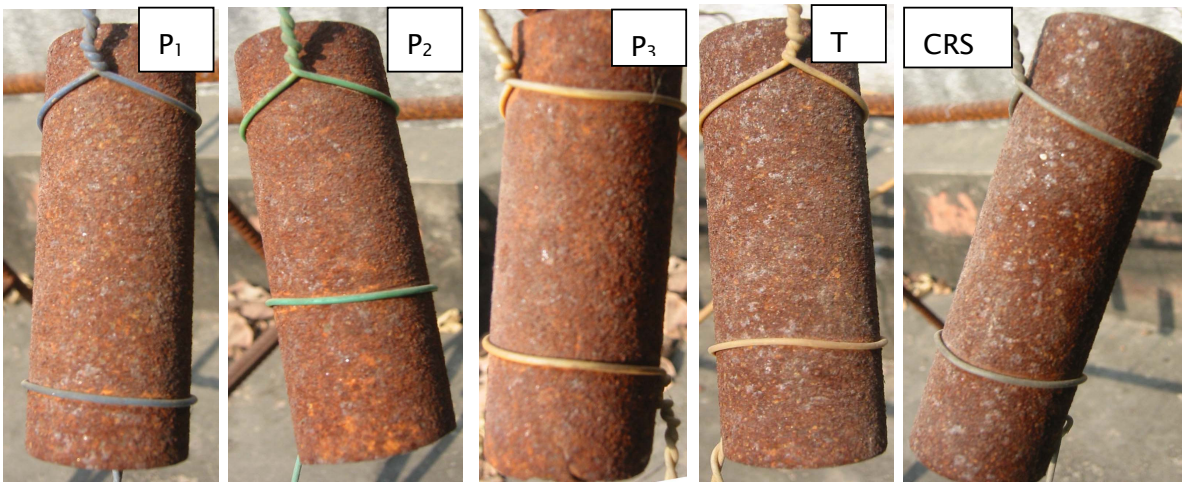


Figure 4: Macro view of the exposed specimen after one year of exposure showing different color of rust on different samples.

The XRD patterns of the rusts were generally diffused and distinct sharp peaks were not observed. As shown in the XRD pattern for the rust sample P3 (Figure 5(a)) and T (Figure 5(b)), the peak broadening occurred in each case towards the lower Bragg diffraction angle end (peak maxima at $\theta \approx 23/2$).

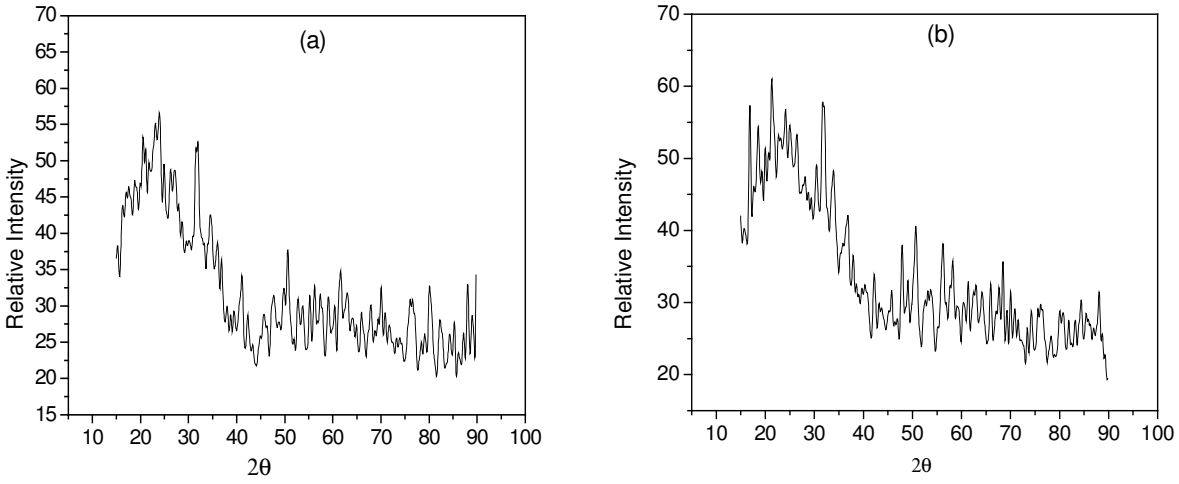


Figure 5: X-ray diffraction spectra of rust sample of: (a) P1 and (b) T

JCSE The Journal of Corrosion Science and Engineering
ISSN 1466-8858 Volume 11, Preprint 11 submitted 30 August 2008

This observation indicated that most of the phases present in the rusts were in the amorphous form.

FTIR spectra of atmospheric rust samples are shown in Figure 6 for $P_1$, $P_2$ and $P_3$, and in Figure 7, for T and C.

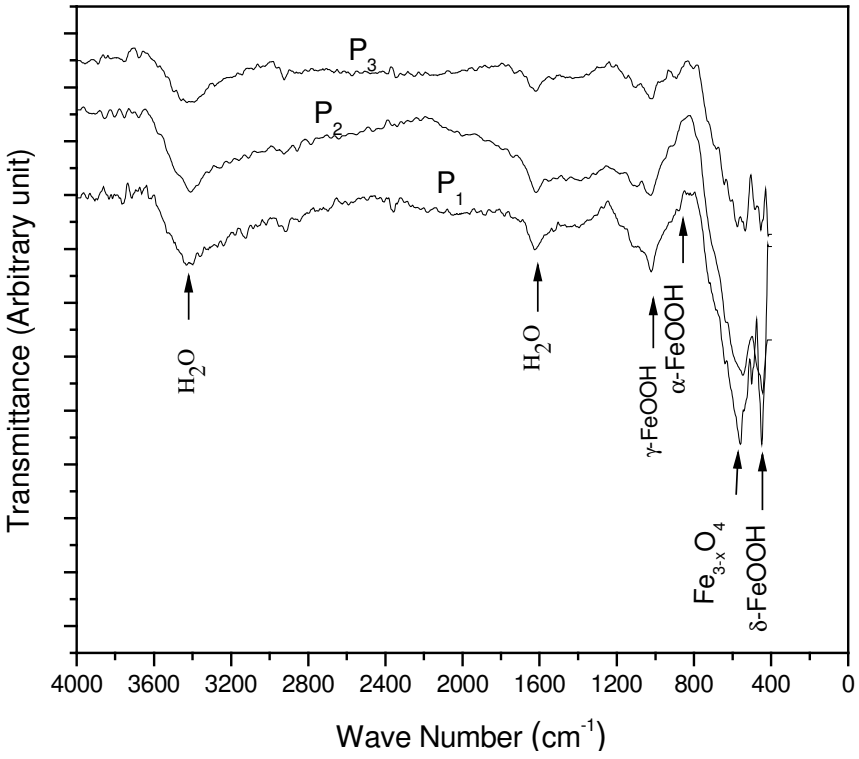


Figure 6: FTIR spectra of rusts from atmosphere exposed samples of P1, P2 and P3.

All spectra appeared to be similar in nature although variations in peak intensities were noted. The phases identified in all the rust samples were γ–FeOOH (lepidocrocite), α–FeOOH (goethite), $Fe_{3-x}O_4$ (magnetite) and δ–FeOOH based on the known characteristic position (wave number) of these phases at 1020 $cm^{-1}$ [7–9], 890 $cm^{-1}$ [7–9], 570 $cm^{-1}$ [10] and 470 $cm^{-1}$ [7–9], respectively. As regard relative abundance, the rusts on phosphoric irons revealed relatively higher amount of δ–FeOOH (see Figure 6 and 7). This is understandable since it is well known that phosphorus in steel/iron catalyses the formation of δ–FeOOH [7]. In case of low alloy steels containing Cu, P and Cr, formation of protective rust composed of $Fe_3O_4$, α–FeOOH, γ–FeOOH and δ–FeOOH has been observed [7–9]. The rust phases identified from FTIR spectra were in conformity with these findings.

JCSE The Journal of Corrosion Science and Engineering
ISSN 1466-8858 Volume 11, Preprint 11 submitted 30 August 2008

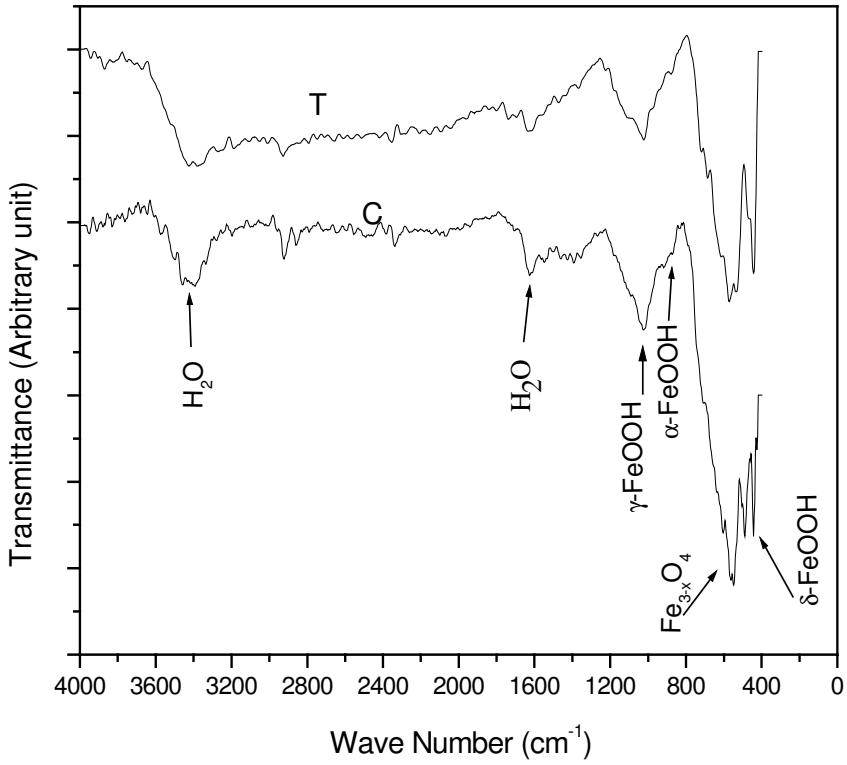


Figure 7: FTIR spectra of rust derived from atmosphere exposed samples of T and C.

After completion of one year of atmospheric exposure, the protective quality of rust was evaluated by Tafel polarization. Figure 8 shows the Tafel plots of rusted samples obtained in aerated, unstirred 3.5 % NaCl solution of pH 6.8. The extended linear Tafel region of cathodic branch indicated that cathodic reaction was activation controlled, in contrast to the expected diffusion controlled $O_2$ reduction in unstirred, aerated 3.5 % NaCl solution. This is probably due to the reduction of $Fe^{3+}$ and $Fe^{2+}$ present in the rust (magnetite and iron oxyhydroxide), which dominates cathodic reaction with almost 100 % current efficiency. The reduction of iron ions as dominant cathodic reaction can be explained using following hypothesis.

The two most important cathodic reactions supporting corrosion are hydrogen evolution ($2H+ + 2e \rightarrow H_2$) and oxygen reduction reaction ($O_2 + 2H_2O + 4e \rightarrow 4OH^-$), which occur either independently or simultaneously [5]. Another cathodic reaction is the reduction of

JCSE The Journal of Corrosion Science and Engineering
ISSN 1466-8858 Volume 11, Preprint 11 submitted 30 August 2008

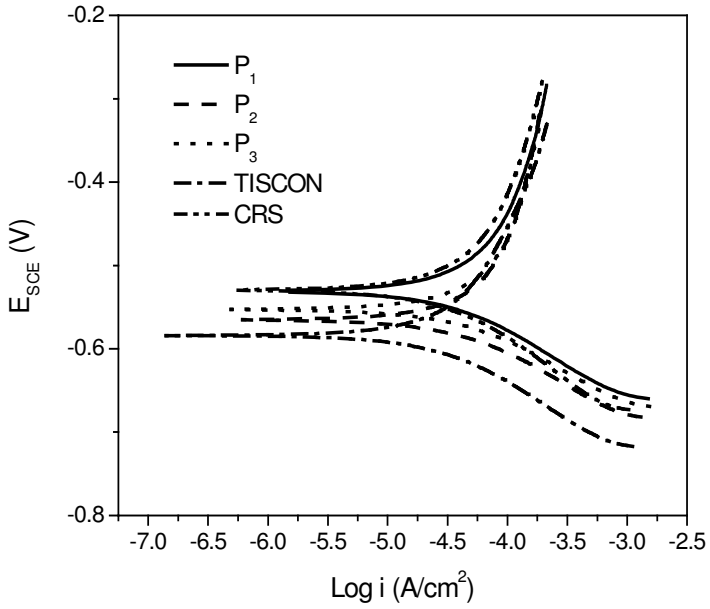


Figure 8: Tafel plots of rusted samples in aerated, unstirred 3.5 % NaCl solution of pH 6.8 obtained at room temperature (250C) using a scan rate of 0.166mV/s.

water ($2H_2O + 2e \rightarrow H_2 + 2OH^-$), which usually occurs at higher overpotential [5]. In general, at low overpotential near to Ecorr, linear Tafel region is observed in the cathodic polarizatio curve, which indicates activation-controlled reaction. At relatively higher over potential when hydrogen ion concentration (active species) approaches zero at the interface of the electrode, a vertical section of the cathodic polarization curve is observed, which indicates diffusion controlled cathodic reaction. However, if the active species or oxidizer is sufficiently available at the interface of electrode, then the cathodic reaction will be activation controlled and hence there will not be present any diffusion controlled vertical section of the cathodic polarization curve. In the present case, it can be hypothesised that the dominant cathodic reaction in 3.5 % NaCl solution is reduction of iron oxide and/or iron oxyhydroxide, which are present at the immediate surface (rust) of the electrode where $Fe^{3+}$ and $Fe^{2+}$ present in the rust can reduce to Fe. This can dominate the other reduction reactions like hydrogen evolution and oxygen reduction. As a result of this the cathodic polarization curve is activation controlled and hence, the extended linear Tafel region was observed. The current efficiency can be determined from the rate controlling step of the cathodic reaction. If the reduction process is activation controlled, i.e. when the oxidizer concentration is sufficiently high, then the oxidizer will dominate cathodic reaction with

ISSN 1466-8858 Volume 11, Preprint 11 submitted 30 August 2008

100 % current efficiency. As iron oxide and/or iron oxyhydroxide present immediately on the surface of the electrode, activation controlled reaction takes place with almost100 % current efficiency.

The corrosion rates estimated from Tafel plots of the rusted samples are provided in Table 2. All samples exhibited similar corrosion rates. The corrosion rates are comparable with corrosion rate of pure iron, obtained by Tafel extrapolation, in unstirred, air saturated 3.5 % NaCl solution, which is 0.304 mm/year [12] and that of plain carbon steel (AISI 1020) which is 0.381 mm/year after one-year immersion in quiet seawater [13].

Table 2: Tafel parameters and corrosion rates estimated from Tafel plots obtained in 3.5 % NaCl

| Sample | βc (mV/dec) | icorr (μA/cm2) | Corrosion rate (mm/year) |
|---|---|---|---|
| $P_1$ | 85 | 29 | 0.330 |
| $P_2$ | 75 | 30 | 0.355 |
| $P_3$ | 79 | 35 | 0.406 |
| T | 99 | 27 | 0.304 |
| C | 90 | 25 | 0.279 |

The anticipated beneficial effect of phosphorus in phosphoric irons towards atmospheric corrosion was not observed during the short period of one year exposure. It is likely that the rust on phosphoric irons may become more protective in nature after more exposure time because it is known that it takes a minimum of three years for the formation of protective rust on the Delhi Iron Pillar [13], a typical phosphoric iron structure.

## 3.2 Salt Spray Test

Similar to the nature of the rust derived from atmospheric test, the XRD patterns of rusts derived from salt spray exposure test were diffused and distinct sharp peaks could not be consistently observed.

JCSE The Journal of Corrosion Science and Engineering
ISSN 1466-8858 Volume 11, Preprint 11 submitted 30 August 2008

FTIR spectra of rusts of phosphoric irons, T and C, derived from continuous salt spray and wet-dry cyclic tests, were similar. The intensity of γ-FeOOH peaks was more in the case of continuous salt spray than that for cyclic wet-dry testing. FTIR spectra of rusts on phosphoric iron $P_1$ derived from continuous salt spray and cyclic wet-dry testing are compared in Figure 9.

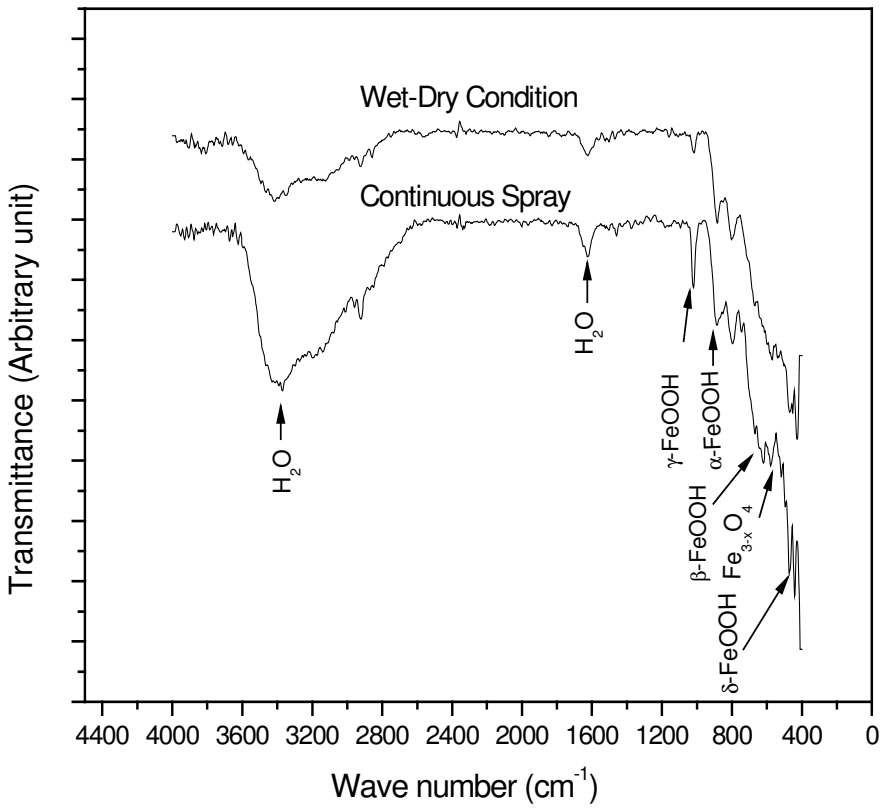


Figure 9: FTIR spectra of rust derived after 15 days of continuous salt spray exposure and 20 days of cyclic wet-dry exposure.

Phases identified in the rust samples of $P_1$, $P_2$, $P_3$, T and C, after both continuous salt spray and wet-dry cyclic tests, were α-FeOOH, β-FeOOH, γ-FeOOH, δ-FeOOH and $Fe_{3-x}O_4$. The notable difference between these rusts and those obtained after atmospheric exposure was the presence of β-FeOOH (akaganiete) in the samples exposed to salt spray. The presence of β-FeOOH was inferred from the peak at around 670 $cm^{-1}$ [14]. The formation of β-

ISSN 1466-8858 Volume 11, Preprint 11 submitted 30 August 2008

FeOOH can be explained by dissolution of iron followed by formation of $FeCl_2$ / $FeCl_3$ hydrolysis products in salt spray derived rusts [15].

On visual observation it was noticed that the rust formed on samples after 15 days of continuous salt spray test was less adherent, while the rusts formed on the samples after 20 days of wet-dry cyclic test were relatively adherent. This could possibly be related to the presence of relatively higher amount of non-protective γ-FeOOH (as revealed by larger peak intensities in FTIR spectra) in the rust obtained after continuous salt spray tests. In contrast, a medium intensity γ-FeOOH peak was observed in case of wet-dry cyclic tests.

The presence of a thick rust layer with medium intensity γ-FeOOH band in FTIR spectra in case of rust obtained from cyclic wet-dry salt spray test can be explained by the following arguments. The studies of Stratmann et al. [16-20] on the corrosion behavior of pure iron under wet-dry cyclic test condition have revealed that during the wet cycle, the cathodic reaction is the reduction of γ-FeOOH to Fe.OH.OH. This Fe.OH.OH containing $Fe^{2+}$, acts as intermediate and is reoxidized to γ-FeOOH again during the drying process. Thus, reoxidized γ-FeOOH works as cathodic site. The dissolution of iron leads to the creation of $Fe^{2+}$ species within the lattice of the γ-FeOOH, therefore increasing the thickness of rust layer in subsequent wet-dry process. At certain negative potential, the free corrosion potential of Fe, γ-FeOOH is reduced to $Fe_3O_4$, which is not oxidized back to γ FeOOH during the drying cycle [21]. This could be the reason of observed medium intensity peak of γ-FeOOH of rusts obtained from cyclic wet-dry test compared to that of rust obtained from continuous salts spray test. In contrast to γ-FeOOH, α-FeOOH is thermodynamically stable and not easily reduced. For this reason, the decrease in corrosion rate has been attributed to the presence of α-FeOOH in rust as main constituent [22]. As the FTIR spectra of phosphoric irons, T and C samples, both in continuous salt spray and cyclic wet-dry tests showed almost similar low intensity α-FeOOH peaks, the rusts were not protective.

## 3.3 EIS studies of Salt Sprayed Samples

EIS experiments were performed after one day and 15 days of continuous salt spray testing and after 20 days of cyclic wet-dry testing. Single time constant impedance response was noticed for all samples in both conditions. The Bode magnitude plots of salt spray exposed specimens of $P_1$, for both conditions, are shown in Figures 10.

JCSE The Journal of Corrosion Science and Engineering
ISSN 1466-8858 Volume 11, Preprint 11 submitted 30 August 2008

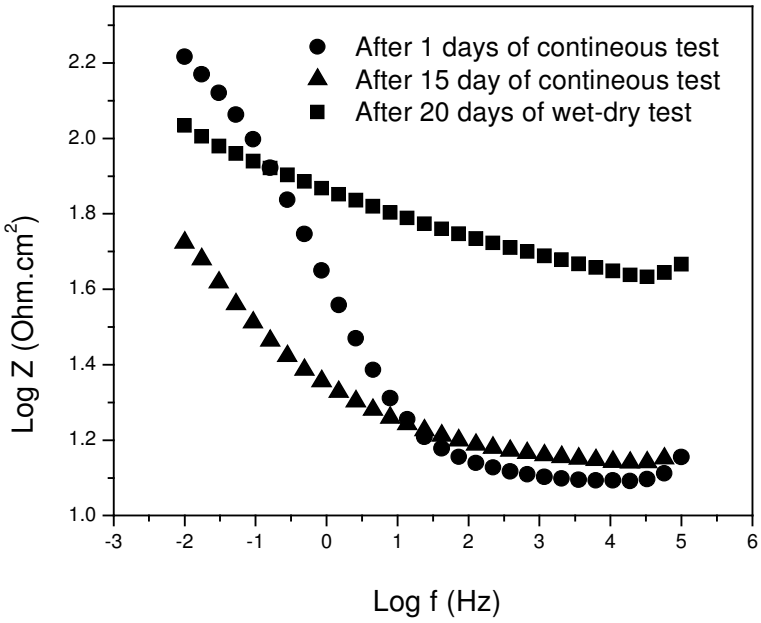


Figure 10: Bode magnitude plots of rusted samples of $P_1$ obtained in 3.5 % NaCl of pH 6.8.

In all cases, the equivalent circuit Rr(QRp) best fit the obtained EIS data, where Rp and Q are polarization resistance and constant phase element, respectively. The Rr and Rp values obtained from modeling of the impedance spectra for all samples are provided in Table 3. There was a fall in polarization resistance with time of testing in continuous salt spray. The Rr of samples after one day and 15 days of continuous salt spray remained almost constant (below 14 Ohm.cm$^2$, Table 3).

In reality Rr is not the solution resistance. The resistance component 'Rr' increased significantly after 20 days of exposure of wet-dry test, in all cases. The enhancement of corrosion of carbon steel is well known in wet-dry environment and is due to electrochemically active species γ-FeOOH formed in dry cycles, which act as strong oxidant in wet cycle [23-28]. This leads to the increase in thickness of rust. Therefore, the significant increase in the resistance in 100 Hz frequency range in wet-dry condition was related to the resistance of pores in the rust (or resistance of solution present in the pores of the rusts) and this is termed as rust resistance (Rr) [24].

JCSE The Journal of Corrosion Science and Engineering
ISSN 1466-8858 Volume 11, Preprint 11 submitted 30 August 2008

Table 3: Parameters Rp and Rr obtained by modeling of EIS data for specimens subjected to wet-dry and continuous salt spray conditions. Rp is the polarization resistance and Rr is the rust resistance.

| Samples | Test type | days | Rr (Ohm.cm$^2$) | Rp (Ohm.cm$^2$) |
|---|---|---|---|---|
| $P_1$ | Continuous spray | 1 | 10 | 150 |
| | | 15 | 14 | 60 |
| | Wet-dry | 20 | 42 | 108 |
| $P_2$ | Continuous spray | 1 | 7 | 135 |
| | | 15 | 12 | 60 |
| | Wet-dry | 20 | 57 | 155 |
| $P_3$ | Continuous spray | 1 | 8 | 130 |
| | | 15 | 12 | 77 |
| | Wet-dry | 20 | 56 | 165 |
| T | Continuous spray | 1 | 11 | 140 |
| | | 15 | 11 | 40 |
| | Wet-dry | 20 | 77 | 135 |
| C | Continuous spray | 1 | 11 | 120 |
| | | 15 | 11 | 55 |
| | Wet-dry | 20 | 70 | 180 |

Rp of samples obtained after 15 days of continuous salt spray testing were significantly lower than those obtained after one-day exposure. After 15 days of continuous spray, Rp of phosphoric irons was higher for higher phosphorus content, and higher than that of C and

ISSN 1466-8858 Volume 11, Preprint 11 submitted 30 August 2008

much higher than that of T. Rp of samples obtained after 20 days of wet-dry testing were higher than that observed for samples after 15 days continuous salt spray testing. Similar to the case of continuous spray, Rp of phosphoric irons was higher with increasing phosphorus content. The Rp of $P_3$ and $P_2$ were higher than that of T. Therefore, the EIS data indicated the beneficial effect of phosphorus in phosphoric irons in resisting attack due to chloride ions. This was in tune with the extensive testing results of the sample in concrete environments containing chlorides [3], where enhanced chloride pitting resistance of phosphoric irons was revealed, when compared to conventional concrete reinforcement steel.

## 4.0 Conclusions

The corrosion products of phosphoric irons (Fe-0.11P-0.028C, Fe-0.32P-0.026C and Fe-0.49P-0.022C, all in wt. %), plain carbon steel (Fe-0.148 C-0.542 Mn-0.128 Si) and a microalloyed steel (Fe-0.151C-0.088P-0.197Si-0.149Cr-0.417Cu) were studied by X-ray diffraction and FTIR techniques after one year exposure to atmosphere, 15 days of exposure to continuous salt spray and 20 days of exposure to of cyclic wet-dry salt spray conditions. The rust components present in the atmosphere exposure rusts were α-FeOOH, γ-FeOOH, δ-FeOOH and $Fe_{3-x}O_4$. The relative amount of δ-FeOOH was higher in case of phosphoric irons compared to conventional steels. In the case of rusts obtained from salt spray testing, β-FeOOH was identified in addition to above rust components. The corrosion rates obtained for atmosphere-rusted surface, by Tafel extrapolation experiment, were also similar in all cases. Electrochemical impedance spectroscopy experiments on salt spray exposed samples, however, indicated the beneficial effect of phosphorus in phosphoric irons in resisting attack due to chloride ions.

## Acknowledgement

The authors acknowledge Tata Steel, Jamshedpur, India for providing reference samples T and C, and Field Gun Factory, Kanpur for forging the phosphoric irons and composition analysis

## References

[1] 'On the Corrosion Resistance of the Delhi Iron Pillar', R. Balasubramaniam,. *Corros. Sci.*, ***42***, pp2103-2129, 2000.

[2] 'Characterization of Delhi Iron Pillar Rust by X-ray Diffraction, Fourier Infrared Spectroscopy, Mössbauer Spectroscopy', R. Balasubramaniam, A. V. Ramesh Kumar,. *Corros. Sci.*, **42**, pp 2085-2101, 2000.

[3] 'Corrosion of Novel Phosphoric Irons for Concrete Reinforcement Applications', PhD Thesis, Indian Institute of Technology, G. Sahoo, Kanpur, India, 2006.

[4] 'Mechanical behaviour of phosphoric irons for concrete reinforcement applications', G. Sahoo, R. Balasubramaniam, *Scripta Mater.*, **56**, pp117-120, 2007..

[5] 'Fundamentals of Electrochemical Corrosion, ASM International', E. Stansbury, R. Buchanan, pp195 and pp116-118, 2000,.

[6] 'Corrosion mechanisms for iron and low-alloy steels exposed to the atmosphere', T.E. Graedel, R.P. Frankenthal, *J. Electrochem. Soc.*, **137**, 2385-2394, 1990.

[7] 'The mechanism of atmospheric rusting and the effect of Cu and P on the rust formation of low alloy steels', T. Misawa, T. Kyuno, W. Suetaka, S. Shimodaira, *Corros. Sci.*, **11,** pp35-48, 1971.

[8] 'The mechanism of atmospheric rusting and the protective amorphous rust on low alloy-steel', T. Misawa, K. Asami, K. Hashimoto, S. Shimodaira, *Corros. Sci.,* **14,** pp.279-289, 1974.

[9] 'The long term growth of the protective rust layer formed on weathering steel by atmospheric corrosion during a quarter of a century,M. Yamashita', H. Miyuki, H. Matsuda, H. Magano, T. Misawa, *Corros. Sci.,* **36,** pp283-299, 1994.

[10] 'Infrared absorption spectra and cation distributions in $(Mn,Fe)_3O_4$', M. Ishii, M. Nakahira, *Solid State Commun.,* **11**, pp209-212, 1972.

[11] 'Validation of corrosion rates measured by the Tafel extrapolation method', E. McCafferty, *Corros. Sci.,* **47,** pp3202-3215, 2005.

[12] 'Handbook of Oceanographic Engineering Materials',S.C. Dexter, John Wiley & Sons, New York, p. 111, 1979.

[13] 'On the growth kinetics of the protective passive film of the Delhi iron Pillar', R. Balasubramaniam, *Current Science,* **82,** pp1357-1365, 2002.

[14] 'The application of IR spectroscopy to the study of atmospheric rust systems I. standard spectra and illustrative applications to identify rust phases in natural atmospheric corrosion products', A. Raman, B. Kuban, K. Razvan, *Corros. Sci.*, **32,** pp1295-1306, 1991.

[15] 'Influence of anions on the formation of β-FeOOH rusts', T. Ishikawa, S. Miyamoto, K. Kandori, T. Nakayama, *Corros. Sci.*, **47,** pp2510-2520, 2005.

[16] 'The mechanism of the oxygen reduction on rust-covered metal substrates', M. Stratmann, J. Müller, *Corros. Sci.,* **36,** pp327-359, 1994.

[17] 'Attempts to understand the course of atmospheric corrosion of iron', M. Stratmann, K. Bohnenkamp, H. J. Engell, *Mater. Corros.*, **34,** pp604-612, 1983.

[18] 'The influence of copper upon the atmospheric corrosion of iron', M. Stratmann, K. Bohnenkamp, T. Ramchandran, *Corros. Sci.,* **27,** pp905-926, 1987.

[19] 'An electrochemical study of phase-transitions in rust layers', M. Stratmann, K. Bohnenkamp, H. J. Engell, *Corros. Sci.,* **23,** pp969-985, 1983.

[20] 'On the atmospheric corrosion of metals which are covered with thin electrolyte layers—II. Experimental results', M. Stratmann, H. Streckel, *Corros. Sci.* **30,** pp697-714, 1990.

[21] Advances in understanding atmospheric corrosion of iron. II. Mechanistic modelling of wet-dry cycles, S. Hoerlé, F. Mazaudier, P. Dillmann, *Corros. Sci.* **46,** pp1431-1465, 2004.

[22] 'Corrosion Current Distributions in a Low-Alloy Steel Covered with a Layer ofRust Formed under Electrolyte Thin Films in a NaCl Solution', M. Yamashita, Y. Yonezawa, H. Uchida, *J. Jpn. I. Met,* **63,** pp1332, **1999**.

[23] 'Composition and protective ability of rust layer formed on weathering steel exposed to various environments', T. Kamimura, S. Hara, H. Miyuki, M. Yamashita, H. Uchida, *Corros. Sci.,* **48,** pp2799-2812, 2006.

[24] 'Effect of Al on the corrosion behavior of low alloy steels in wet-dry environment', T. Nishimura, A. Tahara, T. Kodama, *Mater. Trans.,* **42**, pp478-483, 2001.

[25] 'Quantitative classification of patina conditions for weathering steel using a recently developed instrument', H. Kihira, S. Ito, T. Murata, *Corrosion,* **45,** pp347-352, 1989.

[26] 'Electrochemical Mechanism of Atmospheric Rusting', U. R. Evans, *Nature,* **206,** pp980-982, 1965.

[27] 'The inhibition of the corrosion of iron in the pH range 6-9', D. Gilroy, J. E. O. Mayne, *Brit. Corros. J.,* **1,** pp107-109, 1965.

[28] 'Mechanism of rusting', U. R. Evans, *Corros. Sci.,* **9,** pp813-821, 1969.